ALD Barrier Layer Materials and Configuration and their Effects on Water Vapor Transmission Performance

W.A. Barrow and E.R. Dickey, Lotus Applied Technology, Hillsboro, OR

ABSTRACT

Interest has recently arisen in transparent barrier layers on plastic web deposited by Atomic Layer Deposition (ALD). ALD naturally deposits symmetrical barrier films on both sides of the substrate, unless measures are taken to limit deposition to one side. There has also been some indication that ALD Al_2O_3 barrier layers may degrade in the presence of very high humidity and temperature. It is important to understand if Water Vapor Transmission Rate (WVTR) data for ALD barrier layers is dominated by lag time and if barrier layer degradation plays a significant role. WVTR data for single-sided and double-sided barrier films comprised of Al_2O_3, TiO_2 and combinations of these materials deposited on plastic web in a conventional ALD reactor are presented. To discern the effects of possible barrier layer degradation in high humidity, results for barrier films coated with polymer layers to control humidity exposure after ALD deposition are also presented. Effects of barrier layer material and configuration are summarized and discussed in the context of steady state permeation theory. The resulting implications for high performance, long lasting ALD barrier layers are also discussed.

INTRODUCTION

Interest in the use of ALD films as barriers to moisture and O_2 has been increasing rapidly in recent years. ALD Al_2O_3 has been reported to be an excellent barrier film on plastic web. These reports, however, have involved conventional ALD batch deposition onto stationary substrates [1-7]. In 2009 the first report of ALD barrier deposition in a roll-to-roll web coater appeared [8]. In that case the barrier material was TiO_2. This was later extended to roll-to-roll web coater deposition of ALD Al_2O_3 barrier films [9]. These developments have made the deposition of ALD barrier layers on web commercially feasible.

As development of ALD barrier films has progressed, WVTR results have occasionally appeared somewhat erratic. Further investigation of the performance of single and double-layer barriers has begun to bring the reasons for these erratic results to light. In the case of Al_2O_3 barrier films it has been found that data on double-layer barriers is actually more representative of single-layer barrier performance due to the fact that the barrier layer on the upstream side of the substrate exposed to high humidity and temperature is degraded and contributes little if any barrier properties to the stack after a few hours. In the case of TiO_2 barriers, which turn out to be stable with respect to humidity and temperature, the exact history of the test sample between the time it was deposited and the time it was measured for moisture permeation has a significant effect on the WVTR results. If the sample is stored in room air for a period of time before WVTR measurement, H_2O diffuses into the stack. This moisture then diffuses out through the downstream barrier layer and contributes moisture flux that has not diffused in through the upstream ALD barrier layer during the period of the test. This preexisting moisture in the stack can cause very confusing WVTR results. Owing to this, great care was taken in the present work to keep the ALD barrier test samples stored under dry N_2 between the time they were deposited and the time they were measured.

Another important factor in characterizing ALD barrier films is that the lag time, even for the simple double-layer barrier structures that naturally occur when an ALD film is deposited on a free standing substrate, are very long. Theory predicts lag times on the order of years for such a double-layer barrier stack that has a steady state flux on the order of 0.001 g/m^2/day. This makes it impractical to measure the flux directly on the double-layer barrier stack. This has significant implications for WVTR characterization of samples during process development of barrier layers and for the characterization and quality control of ALD barrier products. In the case of simple double-layer barrier stacks with the two thin film barrier layers sandwiching the substrate, samples can be taken from the coated web and one side can be removed prior to WVTR testing (or one side can be masked prior to deposition on the sampling section of the web). The resulting single-layer WVTR data can then be used to calculate the performance of the double-layer stack. In barrier layer stacks with multiple contiguously deposited layers, characterizing the performance of the stack appears problematic.

ANALYSIS OF H_2O VAPOR LAG TIME AND FLUX

The theoretical analysis of the lag time of water vapor penetration through barrier coated PET carried out here follows the development of Ash, et.al. [10] This analysis is based on the solution of Fick's laws of diffusion with appropriate boundary conditions for stacked planar layers with a fixed relative

 505/856-7188
53rd Annual Technical Conference Proceedings, Orlando, FL April 17–22, 2010 ISSN 0737-5921

humidity on the upstream side of the stack and a sampling gas flow of dry N_2 on the downstream side of the stack. The solution of Fick's laws results in an expression for the flux, $\Phi(x_n,t)$, across the final boundary between the barrier stack and the sampling gas on the downstream side, where x_n is the position of this final boundary on the downstream side. The fluence, or total quantity of water that has passed the final boundary at a time t is then given by

$$Q(t) = \int_0^t \Phi(x_n, t')\, dt' \tag{1}$$

Assuming the flux of water vapor through the barrier stack eventually reaches a steady state, then in the limit of large t, $Q(t) = \Phi_s(t - L)$, where Φ_s is the steady state flux and L is the lag time. The corresponding theoretical expression for L developed by Ash is rather cumbersome and is not displayed here, but was applied to calculate the theoretical lag times discussed below. Since Water Vapor Transmission Analyzers (WVTA) measure the flux of water at a given time, the resulting data must be integrated with respect to time to give the fluence, Q(t). The intersection of the asymptote of Q(t) with the Q(t) = 0 axis then yields the experimental lag time.

The theoretical analysis of the steady state flux, Φ_s, follows the ideal laminate (or series resistance) model as described by Graff, et.al. [11] The resulting expression for steady state flux is

$$\Phi_s = \frac{P_{H_2O}}{\frac{l_1}{D_1 S_1} + \frac{l_2}{D_2 S_2} + \cdots + \frac{l_n}{D_n S_n}}; \tag{2}$$

where P_{H2O} is the vapor pressure of water on the upstream side, l_i is the thickness of the i^{th} layer, D_i is the diffusivity of the i^{th} layer and S_i is the solubility of water in the i^{th} layer. The flux $\Phi(x_n,t)$ is the output of the WVTA instrument, with Φ_s being the value once the readings reach a steady state.

EQUIPMENT AND EXPERIMENTAL DETAILS

Although the primary interest is in ALD barriers deposited in a roll-to-roll web configuration, the ALD barrier test samples for the current work were deposited in a conventional cross-flow ALD reactor. Techniques for producing appropriate test vehicles, particularly single-sided ALD coatings and stacked structures of Al_2O_3 and TiO_2, are better established in the conventional reactors.

Conventional Cross-Flow ALD Reactor

A conventional cross-flow ALD reactor consists of a vacuum chamber held at a specific temperature through which a steady stream of carrier gas flows. An ideal ALD deposition cycle consists of injecting alternating precursors into this gas flow with sufficient dose to fully saturate the surface and any surface topography and with purge times between precursor pulses sufficient to remove all of each precursor from the volume of the reaction chamber before the start of the next precursor pulse. Following the evacuation of the precursor from the volume of the reaction chamber just a monolayer of that precursor is left on all surfaces within the chamber or the monolayer of the previous precursor has been fully reacted to form molecules of the compound being deposited. For Al_2O_3 the precursors are typically trimethylaluminum (TMA) and H_2O. For TiO_2 the precursors are typically $TiCl_4$ and H_2O. The total cycle time at higher temperatures (>200°C) is on the order of 10 seconds. At room temperature, the total cycle time is on the order of 100 seconds and even with this long cycle time fully purging the precursors, particularly the H_2O, is very difficult.

Sample Preparation

Test coupons were cut from rolls of 125 μm and 50 μm thick PET. This PET is industrial grade and was slit and rewound on four inch rolls by a converter. There were no smoothing layers added prior to ALD deposition and the PET was not heat stabilized. Incoming PET rolls were blown off with a hand-held N_2 blow-off gun without unrolling them. The first few feet of each roll was discarded and test samples were cut from the remaining roll material. The test coupons were then blown off again and treated in an O_2 plasma prior to loading into the conventional ALD reactor. No other cleaning processes were used on any of the test samples. The conventional ALD reactor was located in a class 10,000 lab area. No special precautions were taken to reduce particle contamination on the web material during loading of the reactors beyond standard class 10,000 procedures. When the samples were unloaded from the reactor they were immediately stored in a dry N_2 cabinet until they were measured.

Film Characterization

The thicknesses of the Al_2O_3 and TiO_2 barrier films from the conventional cross-flow reactor were assumed to be equal to the thicknesses measured on Si witness coupons that were run together with the PET samples. The film thickness on Si was measured using a Rudolph Research AutoEL III ellipsometer.

Water vapor transmission was measured using commercially available WVTA instruments. Depending on equipment availability and the type of measurements required, either an Illinois Instruments Model 7001 WVTA or a Mocon Aquatran Model 1 WVTA was used. Test coupons were either precut before ALD deposition or cut from strips after ALD deposition using

a template and scalpel. WVTR data were collected at 38°C and 90% RH in the Illinois Instruments 7001 or at 38 °C and 100% RH in the Mocon Aquatran.

Examinations of some barrier films were carried out using a black box and a visible light microscope with phase interference contrast capability. In some cases defects were made visible by applying a drop of concentrated H_2SO_4 to the surface. H_2SO_4 attacks the PET unless the PET is protected by intact barrier film.

RESULTS AND DISCUSSION

Basic Measurement and Analysis of Single Layer Al_2O_3 Barriers on PET

Two single-sided, 64Å, Al_2O_3 barriers on 50 μm PET were produced in a single ALD run. This barrier thickness was chosen to intentionally produce a relatively poor barrier so that WVTR data could be collected in a reasonable period of time. The WVTR for both samples, one in cell A and one in cell B, was measured with the barrier film downstream on the Aquatran instrument until it achieved the steady state. Both samples were then flipped over and measured again with the barrier film on the upstream side. This data is shown in Figure 1. The test with the barrier films on the upstream side was terminated after about three days when it became apparent that the barrier films were almost totally degraded. The Al_2O_3 barriers appear to be stable when only exposed to the moisture flux passing through the PET substrate, but not when exposed directly to 100% RH at 37.8 °C. The steady state flux for the barrier film downstream case for the cell A sample is 0.174 g/m²/day, and for cell B is 0.046 g/m²/day. The significant difference between the two samples from the same ALD run is attributed to several factors. The WVTR vs barrier film thickness is very steep in this thickness range, so very small thickness differences result in large differences in WVTR performance. Other possible contributors are damage during handling and variations in the substrate itself.

To calculate the lag time, L, the fluence, Q(t), was calculated by integrating the flux, Φ(t), with respect to time. The resulting curve for the cell A data with the barrier film on the downstream side from Figure 1 is shown in Figure 2. The asymptote of this curve is then projected back to Q(t) = 0 to obtain the lag time. In this case the lag time is L = 23.7 hours.

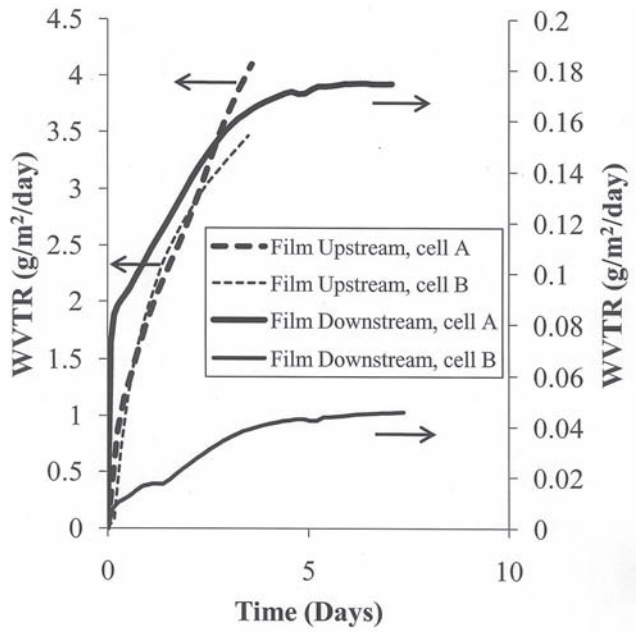

Figure 1: WVTR data for single sided, 64Å Al_2O_3 barrier on 50µm PET (ALD Run # Y2-1447). This barrier was measured first with the Al_2O_3 on the downstream side and then flipped over and measured with the Al_2O_3 on the upstream side. The Al_2O_3 degraded very quickly on the upstream side.

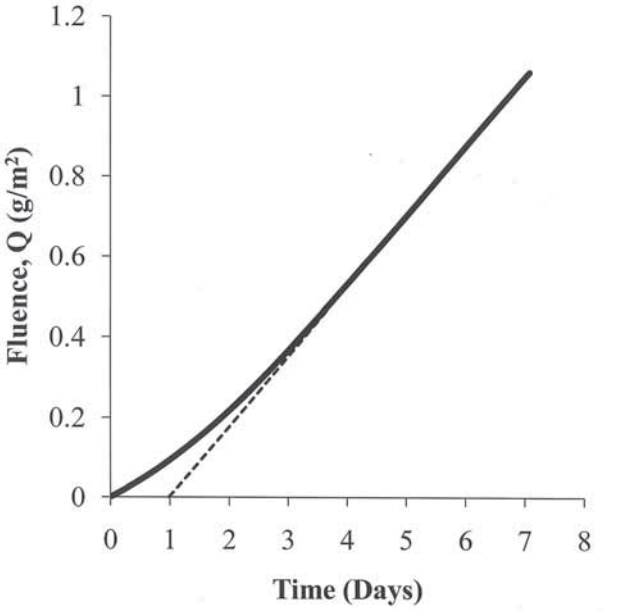

Figure 2: Fluence, Q, for single sided, 64Å Al_2O_3 barrier on 50µm PET (ALD Run # Y2-1447). This curve is the time integral of the downstream data from cell A in Figure 1. The asymptote indicating the lag time as 23.7 hours is also shown.

Fitting this lag time and steady state flux data to the theoretical models requires the selection of several parameters. The physical thicknesses of the PET and the barrier layer are known. The value of the solubility of H_2O in PET of 0.17 g/cm^3/atm was taken from Graff [11]. The value of the diffusivity of H_2O in PET of 4.7×10^{-9} cm^2/sec was chosen by measuring steady state flux and lag time for bare PET and fitting the data to the model. This leaves the solubility and diffusivity of H_2O in the Al_2O_3 layer to be determined. Figure 3 shows families of steady state flux curves as a function of H_2O solubility in Al_2O_3 for various values of H_2O diffusivity in Al_2O_3. Figure 4 shows similar curves for lag time. These curves indicate that the value selected for H_2O solubility in Al_2O_3 and H_2O diffusivity in Al_2O_3 can compensate each other. That is to say, for example, that if the model parameter for H_2O diffusivity in Al_2O_3 is increased by a factor of 10, a decrease in H_2O solubility in Al_2O_3 by a factor of approximately 10 will bring the calculated values of steady state flux and lag time back to where they were. Since neither value is known for the ALD Al_2O_3 films being deposited, the H_2O solubility in Al_2O_3 was taken to be 0.027 g/cm^3/atm, similar to Graff [11], leaving only the H_2O diffusivity in Al_2O_3 as an adjustable parameter in the model.

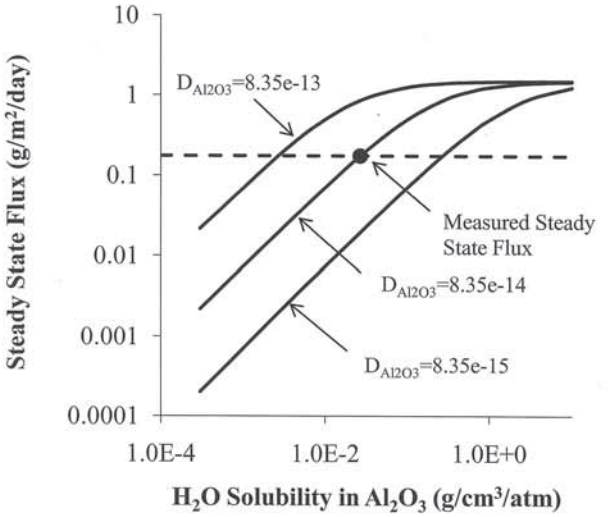

Figure 3: Plot of the family of theoretical steady state flux curves for different H_2O diffusivities and solubilities in Al_2O_3 for the sample from ALD Run # Y2-1447 measured in cell A of the WVTA instrument.

This approach works fine for modeling the steady state flux. Figure 5 shows curves of steady state flux as a function of H_2O diffusivity in Al_2O_3 for various values of PET thickness. A value of H_2O diffusivity in Al_2O_3 of 8.35×10^{-14} cm^2/s produces the correct steady state flux of 0.174 g/m^2/day regardless of the thickness of PET. A problem arises, however, when trying to fit the model to the lag time.

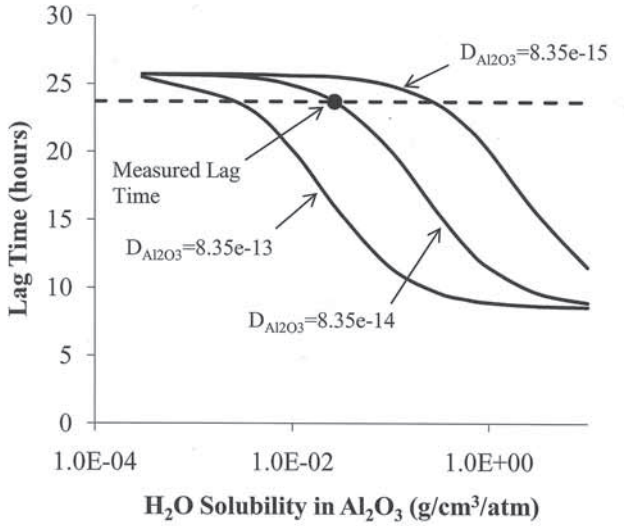

Figure 4: Plot of the family of theoretical lag time curves for different H_2O diffusivities and solubilities in Al_2O_3 for the sample from ALD Run # Y2-1447 measured in cell A of the WVTA instrument.

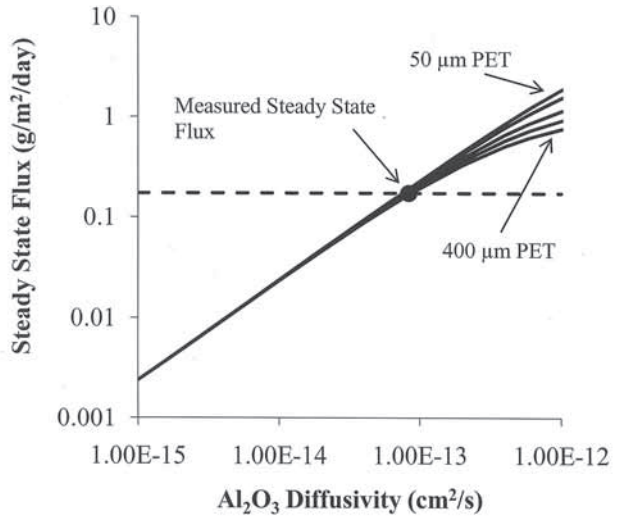

Figure 5: Plot of the family of theoretical steady state flux curves for different effective PET thicknesses and Al_2O_3 diffusivities for the sample from ALD Run # Y2-1447 measured in cell A of the WVTA instrument.

Figure 6 shows the lag time as a function of H_2O diffusivity in Al_2O_3 for various values of PET thickness. It is impossible to fit the lag time value of 23.7 hours with the actual physical thickness of 50 μm of PET. The thickness of PET in the model must be set to 295 μm to get a fit. Graff [11] arrived at a similar conclusion for physical vapor deposited Al_2O_3 barriers based on the failure of an automated root solver routine to fit both steady state flux and lag time without allowing the polymer thickness to vary. They ascribed this to the presence of a distribution of separated defect sites in the barrier layer

through which the moisture had to diffuse, resulting in an increase in the effective path that much of the water had to traverse in the polymer layer.

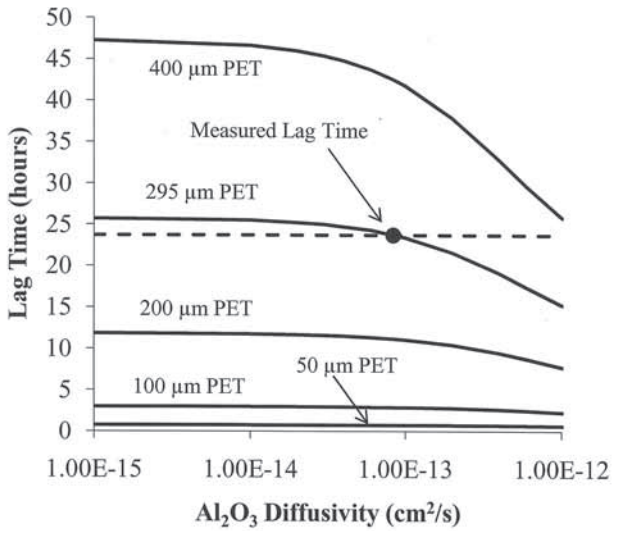

Figure 6: Plot of the family of theoretical lag time curves for different effective PET thicknesses and Al_2O_3 diffusivities for the sample from ALD Run # Y2-1447 measured in cell A of the WVTA instrument.

We were able to find direct evidence for this in the case of our ALD barrier films. Following the WVTR test, a drop of concentrated H_2SO_4 was applied to sample Y2-1447 for 20 seconds. The H_2SO_4 attacks the PET where the barrier layer is not continuous. Figure 7 shows a photograph of this sample taken with an optical microscope after this treatment. Defects are clearly present and they have roughly the spacing expected based on the effective PET thickness of 295 μm needed for the model to fit the lag time.

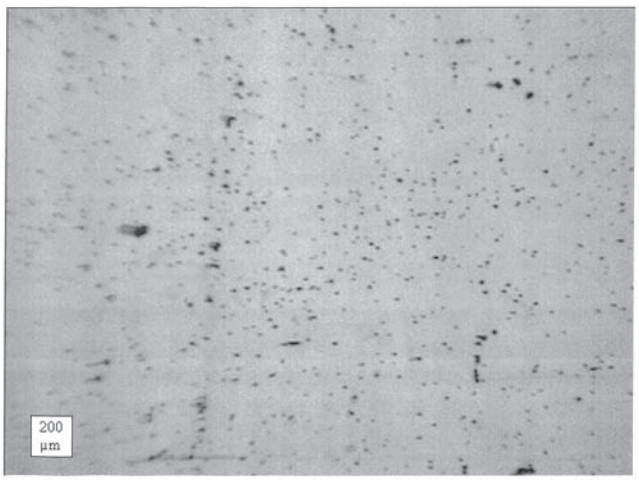

Figure 7: Photomicrograph of single sided, 64Å Al_2O_3 barrier on 50µm PET (ALD Run # Y2-1447) after WVTR testing and application of a drop of concentrated H_2SO_4 for 20 seconds to the Al_2O_3 barrier. The inset square is 200 µm wide to provide a scale reference.

Basic Measurement and Analysis of Single Layer TiO_2 Barriers on PET

Similar tests were carried out on barrier layers of ALD TiO_2 on PET. Figure 8 shows WVTR data for a 71Å thick single-sided TiO_2 barrier layer on 125 μm thick PET (ALD Run # Y2-1473). The steady state flux for the sample in cell A was 0.128 g/m^2/day and the lag time was 70.5 hours. If this data is modeled and the resulting parameters are applied to a corresponding double-sided barrier structure the steady state flux is predicted to be 0.069 g/m^2/day and the lag time is predicted to be 491 hours. The steady state flux for the sample in cell B was 0.177 g/m^2/day and the lag time was 55.6 hours. If this data is modeled and the resulting parameters are applied to a corresponding double-sided barrier structure the steady state flux is predicted to be 0.097 g/m^2/day and the lag time is predicted to be 312 hours.

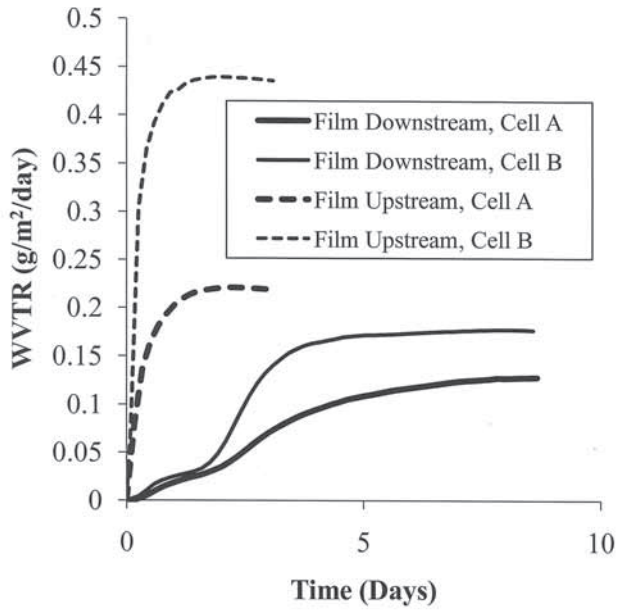

Figure 8: WVTR data for single-sided, 71Å TiO_2 barrier on 125µm PET (ALD Run # Y2-1473). This barrier was measured first with the TiO_2 on the downstream side and then flipped over and measured with the TiO_2 on the upstream side. The TiO_2 film did not appear to degrade on the upstream side.

Moisture Stability of ALD Barrier Films

The most significant difference between the TiO_2 results and the results for Al_2O_3 barrier layers is that in the case of TiO_2 there is no instability found for the barrier layer when exposed directly to high humidity and temperature. Both samples exhibited a large initial flux, presumably due to moisture stored in the stack during the preceding test with the barrier film downstream. They do not, however, exhibit the runaway flux seen in the Al_2O_3 tests with the barrier film upstream. In fact, both samples started to drop back down in the direction of the film downstream results. This result was confirmed separately by exposing much thicker (≈ 700Å) ALD Al_2O_3

and TiO_2 layers on Si substrates to steam. Both samples were suspended directly over a beaker of boiling water. The Al_2O_3 film was completely etched away in less than three minutes. The TiO_2 film was exposed for 4 hours and no changes in optical properties of the film were measureable.

To further explore the issue of stability of the Al_2O_3 barrier films in high humidity, test samples of Al_2O_3 were prepared with thin protective coatings. One sample was 54Å of ALD Al_2O_3 on 125μm PET coated with 2μm of acrylic on top of the Al_2O_3. The other was 45Å of ALD Al_2O_3 coated with 17Å of ALD TiO_2 on 125 μm PET. Both films were tested in the Mocon Aquatran with the barrier films on the upstream side at 100% RH and 38 °C. Both samples exibited runaway flux. Neither of these protective coatings were sufficient to protect the Al_2O_3 barrier layers from attack by moisture. It is not clear based on the data so far whether or not ALD Al_2O_3 barrier layers inside laminated polymer stacks or coated by other materials would be stable to moisture. There is some hope that they might be based on the fact that single-layer ALD Al_2O_3 barrier layers appear to be stable on the downstream side of the the PET substrates.

Characterization of Single-Sided versus Double-Sided Barriers

Characterization of double-sided Al_2O_3 barriers is not useful due to the instability of Al_2O_3 on the upstream side of the stack during measurement. In order to try to produce double-sided ALD barrier films with short enough lag times that measurement times would be practical, very thin TiO_2 barrier layers were deposited. Figure 9 shows WVTR data for both single-sided and double-sided, 50Å thick, TiO_2 barrier layers deposited in the same ALD run. The single sided barrier layers both have steady state fluxes of approximately 0.285 g/m^2/day. The lag time for the sample in cell A is 28.2 hours and for cell B is 24.1 hours. If the single-sided cellA data is modeled and the resulting parameters are applied to a corresponding double-sided barrier structure the steady state flux is predicted to be 0.159 g/m^2/day and the lag time is predicted to be 137 hours. Similarly for cell B the corresponding double-sided barrier structure steady state flux is predicted to be 0.158 g/m2/day and the lag time is predicted to be 127 hours. The measurement of the double-sided, 50Å thick, TiO_2 barrier layers is ongoing. It appears, however, from the data collected so far, that the lag time will be even longer than the theory predicts.

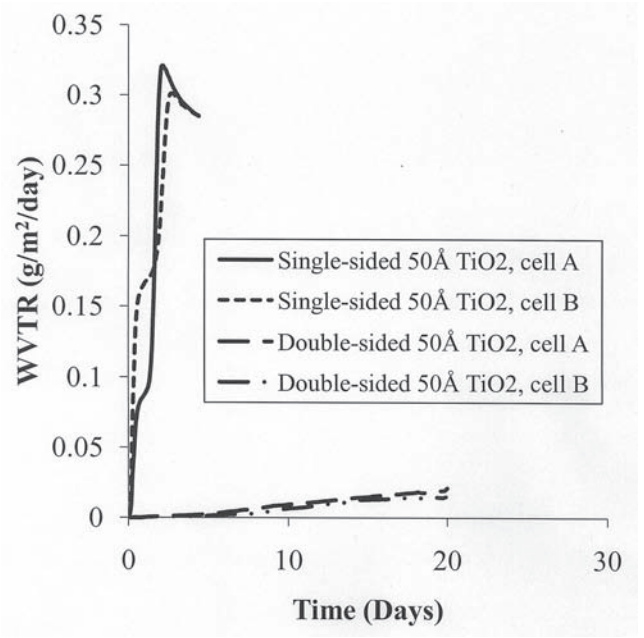

Figure 9: WVTR data for single-sided and double-sided, 50Å TiO_2 barriers on 125µm PET (ALD Run # Y2-1993). The single-sided and double-sided barriers were deposited in the same ALD run.

CONCLUSIONS

Several factors that can contribute to erroneous and confusing ALD moisture barrier performance data have been identified. Accurate WVTR characterization of double-sided ALD barrier layers requires some care in ensuring that the test samples are kept dry until starting the measurement, since moisture can diffuse in through the individual barrier films on each side and build up in the PET relatively quickly as they constitute two single-sided barriers between the atmosphere and the PET. This moisture will then diffuse back out through the downstream barrier film to the sensor and cause spurious readings during the first few days of a WVTR test. A further complication in the case of Al_2O_3 arises when the layer exposed directly to the high humidity side of the measurement system degrades quickly and contributes little if any barrier properties to the stack. In the case of TiO_2 the films are stable with respect to moisture and true double-sided barrier data can, in principle, be measured. The lag time, however, makes direct measurement of even reasonably good double-sided barriers impractical. This has important implications for the characterization and quality control of double-layer barrier structures. For these double-sided ALD barrier structures each ALD barrier film

can be tested on samples from the actual product prior to lamination by removing the layer from one side of a test sample and measuring the remaining layer. Once this has been done for both sides, the performance of the double-layer stack can be estimated. More work needs to be done to better correlate the performance of double-sided and single-sided barriers to improve the accuracy of the lag time and steady state flux estimates for double-sided barriers. A better understanding of the transient behavior of these structures might lead to a better selection of model parameters for the double-sided case.

REFERENCES

1. M.D. Groner, F.H. Fabreguette, J.W. Elam and S.M. George, "Low-Temperature Al_2O_3 Atomic Layer Deposition," *Chem. Mater.*, 16, 639-645, 2004

2. S.-H. K. Park, J. Oh, C.-S. Hwang, J.-I. Lee, Y. S. Yang and H. Y. Chu, "Ultrathin Film Encapsulation of and OLED by ALD," *Electrochemical and Solid State Letters*, 8 (2)1121-1123, 2005

3. A.P. Ghosh, L. J. Gerenser, C. M. Jarman and J. E. Fornalik, "Thin-film encapsulation of organic light-emitting devices," *Applied Physics Letters* 86 223503, 2005

4. M.D. Groner, S.M. George, R.S. McLean, and P.F. Carcia, "Gas Diffusion Barriers on Polymers Using Al_2O_3 Atomic Layer Deposition," *48th Annual Technical Conference Proceedings of the Society of Vacuum Coaters*, pp. 169-172, 2005

5. M.D. Groner, S.M. George, R.S. McLean and P.F. Carcia, "Gas diffusion barriers on polymers using Al_2O_3 atomic layer deposition," *Applied Physics Letters*, 88, 051907, 2006

6. E. Langereis, S.B.S. Heil, M. Creatore, M.C.M. van de Sanden, and W.M.M. Kessels, "Plasma-Assisted Atomic Layer Deposition of Al_2O_3 on Polymers," *49th Annual Technical Conference Proceedings of the Society of Vacuum Coaters*, pp. 151-154, 2006

7. P.F. Carcia, R.S. McLean, M.H. Reilly, M.D. Groner and S.M. George, "Ca test of Al_2O_3 gas diffusion barriers grown by atomic layer deposition on polymers," *Applied Physics Letters*, 89, 031915, 2006

8. E.R. Dickey and W.A. Barrow, "High Rate Roll-to-Roll Deposition of ALD Thin Films on Flexible Substrates," *52nd Annual Technical Conference Proceedings of the Society of Vacuum Coaters*, pp. 38-44, 2009

9. W.A. Barrow and E.R. Dickey, "Roll-to-Roll ALD Deposition of Al_2O_3 Barrier Layers on PET," *Proceedings of the Fall Conference of the Association of Industrial Metallizers, Coaters and Laminators (AIMCAL)*, 2009

10. R. Ash, R.M. Barrer and D.G. Palmer, "Diffusion in multiple laminates," *Brit. J. Appl. Phys.*, 16, 873-884, 1965

11. G.L. Graff, R.E. Williford and P.E. Burrows, "Mechanisms of vapor permeation through multilayer barrier films: Lag time versus equilibrium permeation," *Journal of Applied Physics*, 96(4), pp. 1840-1849, 2004